J. Synchrotron Rad. (1999). **6**, 567–569

The local structure of ferroelectric $Pb_{1-x}Ge_xTe$

Bruce Ravel,[a]* Eric Cockayne[b] and Karin M. Rabe[b]

[a]NIST, Ceramics Division, Gaithersburg MD, 20899 USA, and [b]Dept. of Applied Physics, Yale University, New Haven CT, 06520. E-mail: bruce.ravel@nist.gov

The narrow band-gap semiconductor $Pb_{1-x}Ge_xTe$ has a low-temperature ferroelectric rhombohedral phase whose average structure is a distorted rock salt structure. We have measured the Extended X-ray-Absorption Fine-Structure spectra of $Pb_{1-x}Ge_xTe$ with $x \approx 0.3$ at the Ge and Te K edges and at the Pb L_{III} edge. Guided by first-principles calculations, we create a model for the the local structure as a distortion from the ideal rock salt structure. By co-refining the spectra from these three edges, we demonstrate that the data are consistent with our fitting model. Our results show the power of using first-principles calculations in conjunction with EXAFS measurements to determine local structures in complex materials.

1. Introduction

Ferroelectric solid solutions are of theoretical and experimental interest as well as of significant technological importance. Understanding the physics of these materials requires understanding the local structure. Recent advances both in Extended X-ray-Absorption Fine-Structure (EXAFS) spectroscopy and in first principles calculations give methods for computing and measuring local structures in ferroelectric materials. $Pb_{1-x}Ge_xTe$ is a good prototype for these studies, because the structure and physics of the ferroelectric phase are relatively simple and are known to be dominated by the off-center displacements of Ge ions with respect to their near-neighbor Te octahedra. (Islam & Bunker, 1987)

In this work, we present an approach for measuring the local structure of ferroelectric $Pb_{1-x}Ge_xTe$ that combines theoretical first-principles local density-functional theory (LDFT) calculations with experimental Extended X-ray Absorption Fine Structure (EXAFS) spectroscopy. The average structure of the paraelectric high-temperature phase in $Pb_{1-x}Ge_xTe$ is rock salt as shown in Fig. 1. For $x > 0.005$, the low-temperature phase is ferroelectric, with a rhombohedral unit cell only slightly distorted from cubic ($\alpha \approx 90°$). Phenomenological models for the paraelectric–ferroelectric transition in $Pb_{1-x}Ge_xTe$ are based on Ge off-center displacements. (Islam & Bunker, 1987) In these models, individual Ge ions become more stable by moving from their nominal lattice positions in one of the cubic ⟨111⟩ directions. Below the transition temperature T_c, there is long-range order in the *direction* of off-center displacement of the Ge ions, resulting in a net ferroelectric moment in the crystal. Above T_c, there is no long-range order in the direction of the off-centering, thus the material is paraelectric. Previous EXAFS work (Islam & Bunker, 1987) observed large displacements of the Ge ions both below and above the rhombohedral to cubic phase transition, supporting this phenomenological viewpoint.

Our goal in this work is to provide a more detailed description of the local structure in the ferroelectric phase of $Pb_{1-x}Ge_xTe$. We used a sample with $x \approx 0.3$ ($T_c \approx 360$K) and collected data from the Ge and Te K edges and the Pb L_{III} edge at four temperatures between 40 K and 200 K, all within the low temperature phase. The data were all measured in the transmission geometry and in a Displex cryostat which provided temperature stability to within ±2 K. We exploit advances in theoretical and analytical tools developed in the years since the earlier work (Islam & Bunker, 1987) to provide a more complete picture of the local structure of this material, including secondary distortions not included in earlier models.

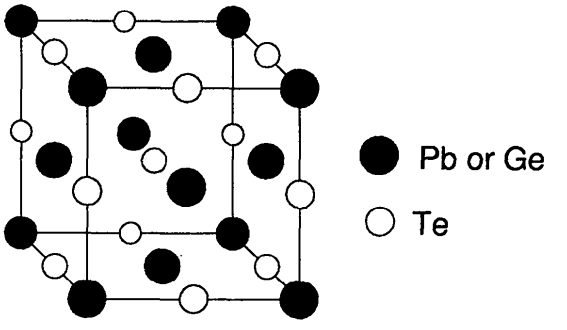

Figure 1
The cubic rock salt structure forms the basis of the local structure of $Pb_{1-x}Ge_xTe$. In the real material, the Ge ions randomly populate the sites with black circles. In the LDFT calculations, these sites are populated by Ge ions in an ordered manner consistent with the supercells shown in Cockayne & Rabe (1998*a*).

2. Theory

Cockayne and Rabe have made LDFT studies (Cockayne & Rabe 1997, 1998*a*,*b*) of several ordered supercells of $Pb_{1-x}Ge_xTe$ at $x = 0.25$ in order to study the effect of the local environment on structural, ferroelectric and piezoelectric properties. The LDFT ground state structures can be used to predict the ground state structure of disordered $Pb_{1-x}Ge_xTe$ at the same composition. In this model, the displacement of any ion from its ideal rock salt position depends on the identity of the nearby cations (Pb or Ge).

Some simplifications of this model are based on physical considerations. The bonding in $Pb_{1-x}Ge_xTe$ is largely the covalent bonding of p orbitals of Pb, Ge and Te. (Littlewood, 1984) We thus, to lowest order, express the displacement of each ion along each Cartesian direction as an additive function of displacements determined only by the identity of the closest cations along that direction. Furthermore, we assume in the model that all Ge ions are displaced from their nominal positions into the [111] octant. With these assumptions, the fully relaxed positions of the ions in any configuration are fully determined by a small set of parameters.

We determine the distortion parameters by a least-squares fit of ionic displacements in LDFT calculations of several Pb_3GeTe_4 supercells as a function of local cation environment in these cells. The model presented here is based on the the four largest calculated distortion parameters. It reproduces the LDFT ground state ionic positions well and is thus predicted to extrapolate to experimental disordered $Pb_{1-x}Ge_xTe$ systems of similar composition. The first is the size of the Ge off-center displacement g. The second is Te relaxation. Te is found to relax an amount r toward the neighboring Ge ion whenever there is a linear Ge–Te–Pb segment, because of the small size of the Ge ion compared to the Pb ion. The third parameter is the coupling of Ge off-centering to Te relaxation. When

a Te relaxes toward a Ge, the corresponding component of Ge off-center displacement is reduced by an amount c. Finally, when a Ge atom moves off-center, other atoms must respond to preserve the center of mass of the system. This movement is mainly Te recoil t opposing the Ge off-centering g in each Ge–Te–cation segment. The LDFT values for the parameters g, r, c and t are given in Table 1. The corresponding amount of displacement of Ge and Te ions in the model for the various local environments are given in Table 2.

3. Data Analysis

The absorption data $\mu(E)$ was converted to the fine structure spectrum $\chi(k)$ using the AUTOBK program (Newville *et al.*, 1993). The most sensitive parameter in AUTOBK is the cutoff in R-space defining the spectral content of the background spline. In each case, this cutoff was chosen to maximize the number of knots available for the background spline without having the knot values be highly correlated with the variable parameters used in the subsequent fits. By maximizing the number of knots, the background spline can more faithfully approximate the true background function. The degree of correlation with the fitting parameters was determined by further refining the background spline with the program FEFFIT (Newville *et al.*, 1995) while simultaneously fitting the $\chi(k)$ data in the manner described in the following paragraphs. In each case we chose the cutoff such that it was as large in R as possible without having the absolute value of the correlation (Newville *et al.*, 1995) between any background spline parameters and any fitting parameter be more than 0.5.

The structural model from the LDFT calculations can be tested against the EXAFS data using theoretical fitting standards from the program FEFF6 (Zabinsky *et al.*, 1995) and the sophisticated model building capabilities of FEFFIT. FEFFIT allows co-refinement of multiple data sets as well as casting the terms in the EXAFS equation as algebraic expressions dependent upon generalized fitting parameters. In this work, we co-refined measurements of all three edges at each temperature. For each fit, we used the model building capabilities of FEFFIT extensively.

Table 1

Distortion parameters in units of half the lattice constant. The theoretical values come from fits to fully relaxed ordered supercells. The measured results come from the co-refinement of the EXAFS at the three edges and are the average of the values found at four temperatures.

param.	description	LDFT	measured
g	Ge off-center displacement.	0.061	0.105(17)
r	Relaxation of Te toward Ge in each Pb–Te–Ge segment.	0.042	0.051(3)
c	Coupling of Ge off-centering to Te relaxation.	0.021	0.037(5)
t	Te recoil due to the Ge off-centering.	0.019	0.016(8)

Table 2

Local configurations and displacement from nominal position of Ge and Te ions in the low-temperature model for $Pb_{1-x}Ge_xTe$. The configurations are the four possible arrangements of ions along any Cartesian directions about either the Ge or Te ions. The displacement of the Ge or Te ion in the positive direction is given in terms of the parameters in Table 1. The net vector displacement of each Ge and Te is the superposition of the displacements due to the chain configurations in each Cartesian direction.

Te config.	displacement	Ge config.	displacement
Pb–Te–Pb	0	Pb–Te–Ge–Te–Pb	$g-2c$
Pb–Te–Ge	$-t+r$	Pb–Te–Ge–Te–Ge	$g-c$
Ge–Te–Pb	$-t-r$	Ge–Te–Ge–Te–Pb	$g-c$
Ge–Te–Ge	$-2t$	Ge–Te–Ge–Te–Ge	g

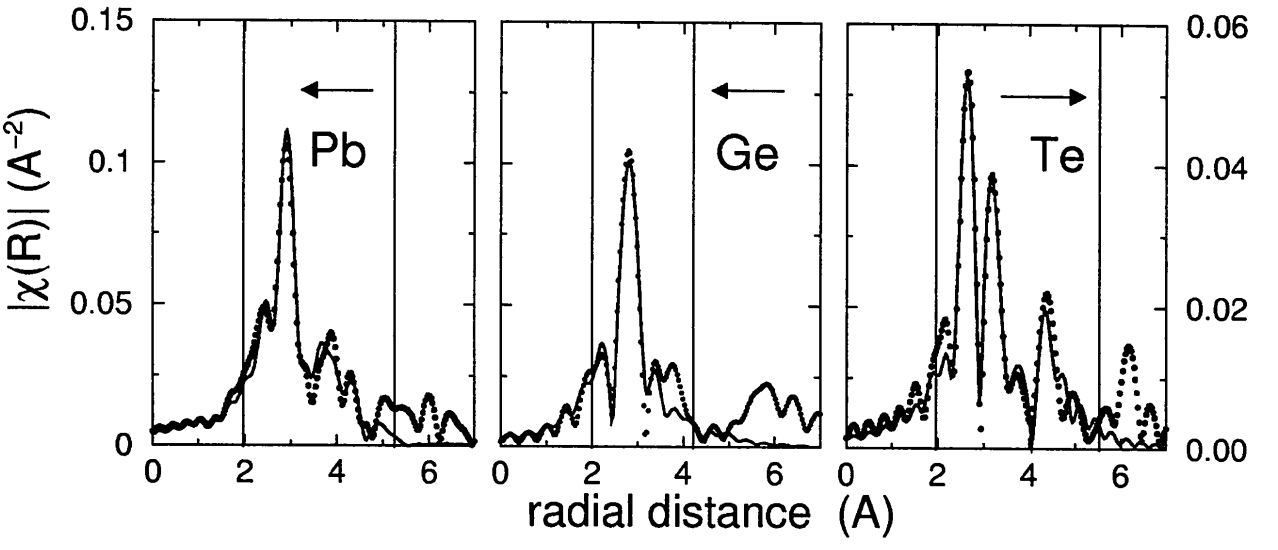

Figure 2

Result of the co-refinement of the Ge and Te K edges and the Pb L_{III} edge EXAFS at 100 K. The magnitudes of the Fourier transforms of the data (points) and the best fits (lines) are shown. The vertical lines indicate the fitting ranges and the arrows indicate which y-axis is appropriate to each plot.

As usual, LDFT underestimates the lattice constant of $Pb_{1-x}Ge_xTe$. Rather than use the LDFT ground state lattice constant of 6.28 Å, we use the temperature dependence of the lattice constant (Hohnke *et al.*, 1972) as a constraint at each temperature. The use of the measured lattice constant as a constraint is justified as the fitting model describes the local structure in terms of distortions away from the rock salt structure. The parameters from Table 1 are then used to describe the pair distribution functions as histograms for each shell around each absorber by evaluating the net displacements of each ion in every possible local configuration as described in Table 2. The location in radial distance of each bin in each histogram depends upon the values of the lattice parameter and of the four distortion parameters. The height of each bin depends on the symmetry of the rock salt structure and the value of the doping fraction, assuming random distribution of Ge ions. As the doping fraction for our sample was known from X-ray diffraction, it and therefore the bin heights in the pair distribution histograms were fixed in our analysis. The locations of the bins are calculated from the values of the lattice and distortion parameters. The fits included single scattering to the third shell, ~ 5.3 Å, around Pb and Te and to the second shell, ~ 4.2 Å, around the Ge. By measuring out to those radial distances, we considered a total of 161 bins in the three pair distribution functions.

These structural parameters along with an appropriate set of amplitude reduction factors S_0^2, phase corrections E_0, and thermal disorder parameters were the variables in our analysis. An S_0^2 was assigned to each absorbing atom. To accommodate for known inadequacies in the potential model used in FEFF, we used E_0 corrections in the manner described in Haskel *et al.* (1995). The thermal disorder parameters were expressed as mean square displacements in bond length. One such parameter for shell or species within a shell was used. Although this amounts to a large number of variables, the use of the model inspired by the first-principles calculations makes this fit tractable. The pair distribution functions for most shells are poorly described by Gaussians. In fact, the first shell about the Ge absorber is split into three distinct peaks. Describing these distribution functions in terms of cumulant expansions would require an inordinate number of fitting variables.

At each temperature, the data from all three edges were corefined using the structural model described above. The great advantage of corefinement is that many parameters are common to the data from two or all three of the edges. For example, the structural parameters described in Table 1 are common to all three edges and most of the parameters describing the mean square variation in bond lengths are common to two data sets. Using data from a variety of temperatures, we can check the reasonableness of several parameters, including the S_0^2 and E_0 parameters which should not change with temperature and the mean square bond length variations, which should show the behavior of a single frequency oscillator (Stern & Heald, 1983).

The result of the fit at 100 K is shown in Fig. 2. This shows that the data is consistent with the distortion model from the LDFT calculation of the structure of $Pb_{1-x}Ge_xTe$. The best fit values of the distortion parameters are shown in Table 1. The fitted values for the distortion parameters showed no temperature variation outside of their uncertainties, thus the values reported in Table 1 are the average values from the four temperatures. The calculated values for the distortion parameters agree fairly well with the measured values, although three of the measured values are larger suggesting that there is more distortion in the real material than is predicted from LDFT relaxation of ordered supercells. This may be due in part to the use of the local density approximation (LDA) in the first-principles calculations. The LDA leads to a lattice parameter for $Pb_{1-x}Ge_xTe$ that is smaller than the experimental one used in the fits to the EXAFS data. First principles calculations show that the Ge off-center displacement parameter g is strongly coupled to the lattice parameter a, increasing as a increases. (Cockayne & Rabe 1997, 1998*b*) The values for S_0^2 for Pb and Ge were consistent within their uncertainties with calculations from FEFF (Zabinsky *et al.*, 1995). The measured Te S_0^2 was somewhat larger. The values for the E_0 parameters were all small and unvarying between temperatures. The Einstein temperatures of the measured bonds were all between 55 and 225 K — reasonable values for such an open structure.

4. Conclusion

In this work, we have determined the local structure of ferroelectric $Pb_{1-x}Ge_xTe$ for $x \approx 0.3$. The use of first-principles theory as a basis for analysis of the EXAFS was essential due to the complexity of the $Pb_{1-x}Ge_xTe$ structure. Using this theory, we were able to parameterize the structure with a small number of physically meaningful fitting variables. This approach also relied heavily on the use of theoretical fitting standards from FEFF and the sophisticated model building capabilities of FEFFIT. We suggest that the union of first principles theory and EXAFS analysis can be widely applicable to problems in materials science, particularly those involving structurally complicated materials.

We thank B. Bunker for providing the $Pb_{1-x}Ge_xTe$ sample, D. Haskel, C.E. Bouldin, J.O. Cross, and J. Woicik for help collecting data, and M. Newville for modifying FEFFIT to accommodate our needs. We are grateful to U. V. Waghmare for guidance in the first-principles calculations. This work was supported in part by the National Research Council and by Office of Naval Research grant #N00014-97-J-0047.

References

Cockayne, E. & Rabe, K. M. (1997). *Phys. Rev. B*, **56**(13), 7947–7961.

Cockayne, E. & Rabe, K. M. (1998*a*). In *First-Principles Calculations for Ferroelectrics*, edited by R. E. Cohen, AIP Conference Proceedings 436, pp. 71–80. Woodbury, NY: American Institute of Physics.

Cockayne, E. & Rabe, K. M. (1998*b*). *Phys. Rev. B*, **57**(22), R13973–R13976.

Haskel, D., Ravel, B., Newville, M. & Stern, E. (1995). *Physica B*, **208&209**, 151–153.

Hohnke, D., Holloway, H. & Kaiser, S. (1972). *J. Phys. Chem. Solids*, **33**, 2053–2062.

Islam, Q. & Bunker, B. (1987). *Phys. Rev. Lett.* **59**(23), 2701–2704.

Littlewood, P. B. (1984). *CRC Crit. Rev. Solid State Mater*, **11**, 229.

Newville, M., P. Līviņš, Yacoby, Y., Rehr, J. J. & Stern, E. A. (1993). *Phys. Rev. B*, **47**(21), 14126–14131.

Newville, M., Ravel, B., Haskel, D., Rehr, J. J., Stern, E. A. & Yacoby, Y. (1995). *Physica B*, **208&209**(1–4), 154–156.

Stern, E. A. & Heald, S. M. (1983). In *Handbook of Synchrotron Radiation*, edited by E. E. Koch, pp. 995–1014. New York: North-Holland.

Zabinsky, S. I., Rehr, J. J., Ankudinov, A., Albers, R. C. & Eller, M. J. (1995). *Phys. Rev. B*, **52**(4), 2995–3009.

(Received 10 August 1998; accepted 18 November 1998)